

A STUDY ON THE BEHAVIOR OF A SEISMIC ISOLATION DEVICE USING FULL-SCALE DYNAMIC PUSH-OVER EXPERIMENTAL EQUIPMENT

by

Takashi SATOU¹⁾, Hiroshi MITAMURA²⁾, Akio HAYASHI³⁾, Toshihiko BESSYO⁴⁾

ABSTRACT

Seismic isolation bearings of steel were developed for use in cold regions. They were designed to use the friction between polytetrafluoroethylene and steel and the geometric shape without using rubber. From the histeresis curves, seismic isolation bearing of steel that uses very large values of friction yield histeresis reduction, and to reduce natural free vibrations of a structure. It also has an effect of reducing such an impact inertia force that was generated by the equipment used in our experiment.

KEY WORDS

: Seismic isolation bearings of steel
Full-scale
Dynamic push-over experimental equipment
Histeresis reduction

1. FULL-SCALE DYNAMIC PUSH-OVER EXPERIMENTAL EQUIPMENT

We have developed a full-scale dynamic push-over experimental equipment that can generate inertia forces reaching the ultimate limit, using an almost full-scale model of a bridge as a model structure.

1.1 Objective and idea

The Hyogo-ken Nanbu Earthquake on January 17, 1995, caused the greatest damage to various structures, since the Great Kanto Earthquake in 1923. Many bridges sustained serious damage, including the collapse of piers and girders. This experience let to a great change in design of highway bridges, and provision has been established that seismic motions of great intensity has to be taken into account, although the probability of such severe earthquakes occurring while the bridges are in service is little. To consider the seismic motions caused by inland earthquakes directly above their hypocenter in the magnitude 7 class, like the 1995 Hyogo-ken Nanbu Earthquake, the seismic motion of L2 type II was set up. Such an earthquake motion is extremely rare but has a great impact on structures. The motions of this type have an impact

-
- 1) Engineer, Structures Section, Structures Division, Civil Engineering Research Institute, Hokkaido Development Bureau, 1-3 Hiragishi, Toyohira-ku, Sapporo, 062-8602, Japan
 - 2) Research Engineer, ditto
 - 3) DE, Pacific Consultants Co.
 - 4) Engineer, Muroran Plant The Japan Steel Works, LTD.

marked by short duration and a small number of cycles. Figure-1 shows the response spectrum, together with the seismic motions of the previous L2 type I.

To ensure the safety of bridges, the precision and validity of design calculations must always be verified. To guarantee the validity of design calculations, experiments are required in which an almost full-scale model of a planned structure and equipment that can faithfully reproduce seismic motions from design conditions are necessary. A conventional shaking table requires a sizable power unit and a control device to

cause a sudden inertia force to act on full-scale model structures, and separately developed devices are needed to provide the needs of different designers.

Furthermore, the free vibration components of the behavior of a structure subject to seismic motions with an impact marked by a short duration and a small number of cycles are not so large, as typically shown by push-over analysis or the energy conservation law. From these viewpoints, we propose full-scale dynamic push-over experimental equipment.

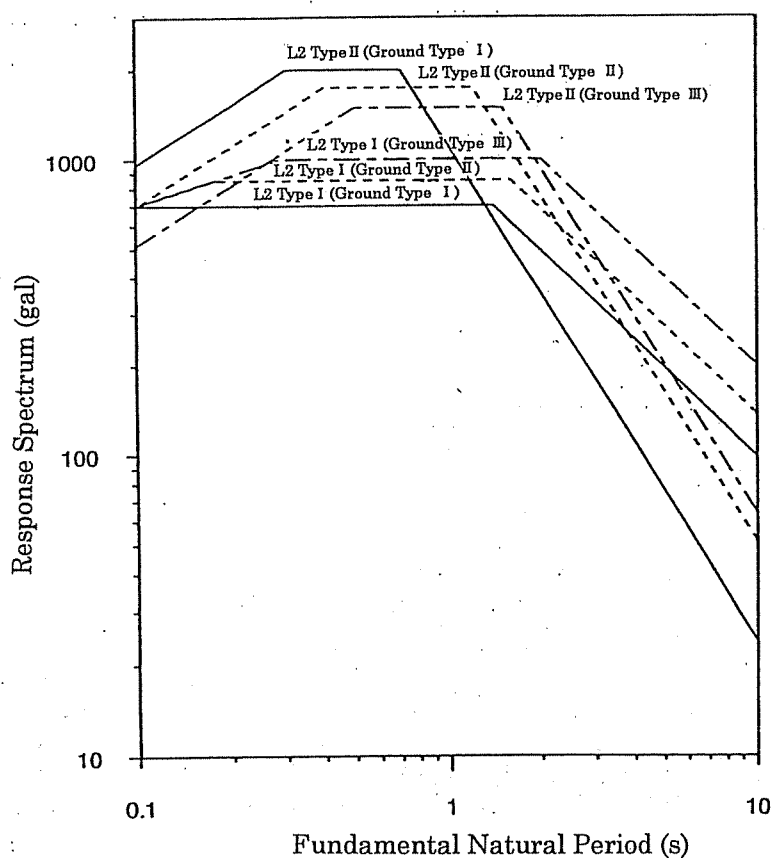


Figure-1 Response Spectrum

1.2 Construction and operation principle

Our proposed equipment operates in the following way: an almost full-scale model of a planned bridge is placed on a pallet. The pallet is raised by air bearings and accelerated. Then the pallet collides against an abutment test wall. The model structure and the pallet generate a great acceleration in the process of making a sudden stop. After this, free vibration, that is, the characteristic vibration of the model structure, occurs. Because making the first acceleration as moderate as possible is needed, equipment consisting of cables and a weight is used (Figure-2). The section where the collision takes place was

provided with a shock absorber of expanded plastics and a rubber plate. The vibration was adjusted by changing the acceleration distance and the thickness of the shock absorber.

Equipment of this kind can reproduce the behavior of a structure subjected to seismic motions with a very noticeable shaking. But it is not useful for the behavior of a structure subjected to seismic motions with a long duration of vibration. However, it is considered to be effective in studying, at limited expense, the effects of impact motions characterized by short duration and a small number of cycles. Figure-3 shows the full-scale dynamic push-over experimental equipment.

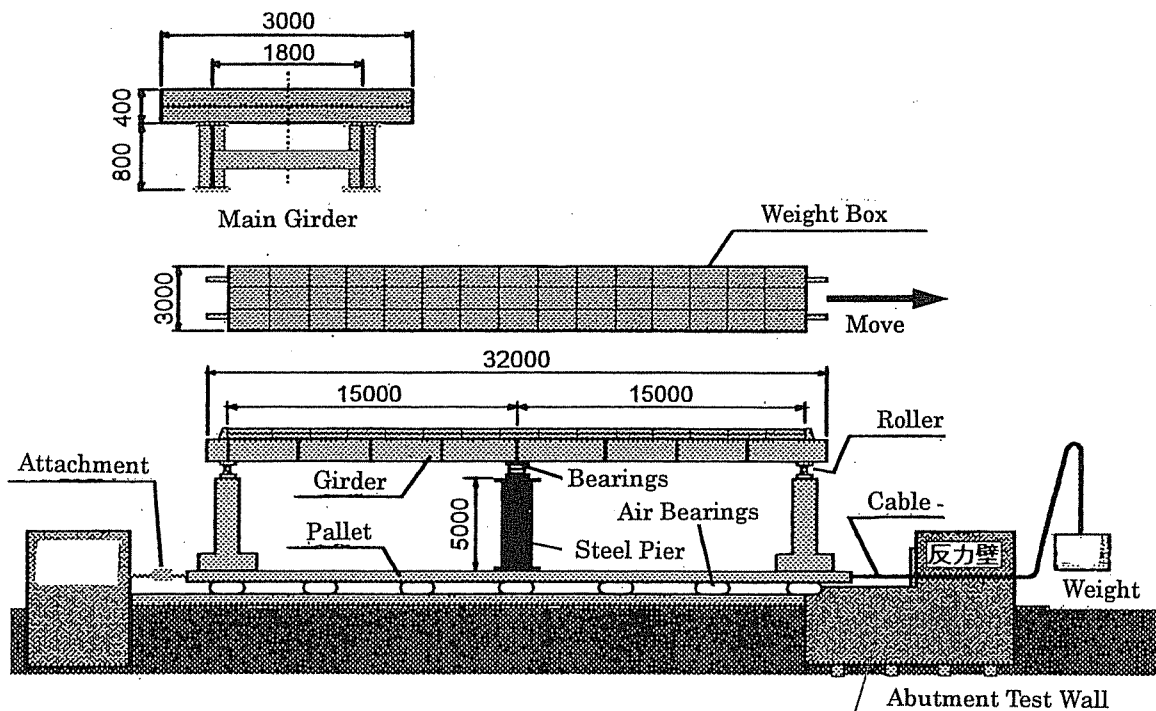


Figure-2 Whole of Experimental Equipment

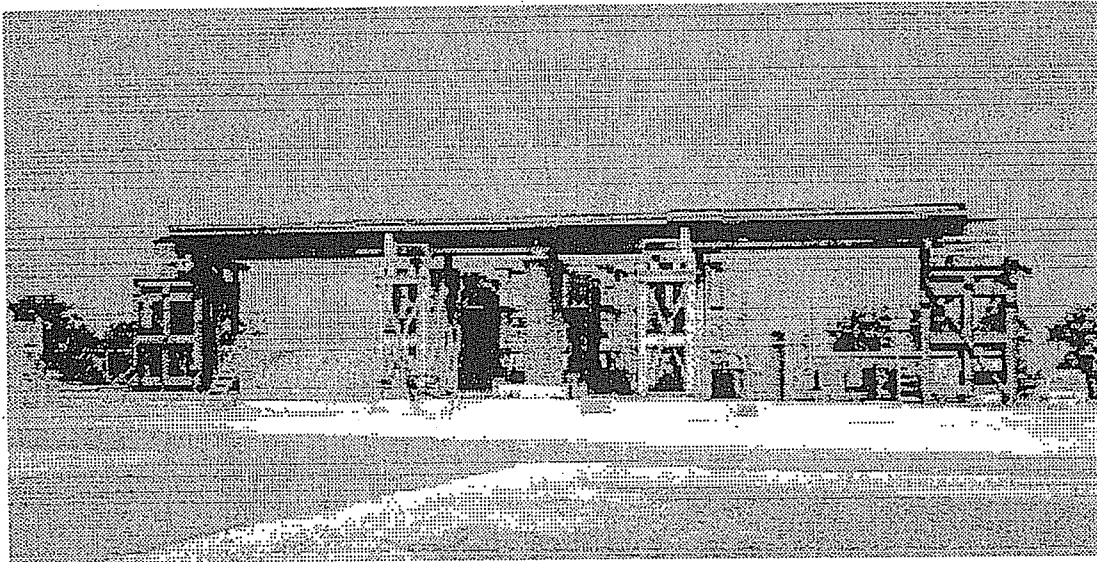


Figure-3 Whole View Picture of Experimental Equipment

2. SEISMIC ISOLATION BEARINGS OF STEEL

2.1 Purpose and details of development

Seismic isolation bearings of steel were developed for use in cold regions. They were designed to use the friction between polytetrafluoroethylene and steel and the geometric shape without using rubber.

Rubber materials harden under cold temperatures. Consequently, seismic isolation devices that have been designed based on characteristics at ordinary temperature can not show the initial performance under cold conditions. This point may be factored into the design of seismic isolation devices, but considerable constraint will be put on the seismic isolation design when the severe motions described in section 1.2 are in the design conditions.

Therefore, isolation devices whose restoring force characteristics do not vary with changes in temperature should be

developed for use in cold regions. We propose seismic isolation bearings of steel as isolation devices that can fulfil this purpose. Figure-4 shows the shape of this device, which uses the friction between polytetrafluoroethylene and steel and the geometric form. That is, this device makes the same movement as the structure formed by linking Points K and K' (Figure-4), and flexibility of behavior and good energy absorption performance can be attained by properly selecting the diameter of the rotating part of the rotor in the center of the device. Furthermore, because the rotor in the center of the device behaves counter to the relative displacements of the upper and the lower shoes, the sliding plane provides a double. As a result, a frictional force representing a friction coefficient twice as large as the normal friction coefficient can be attained. Thus the hysteresis curves of the seismic isolation device were modeled as a bilinear model that was very effective in absorbing energy (equations (1) to (5), Figure-5).

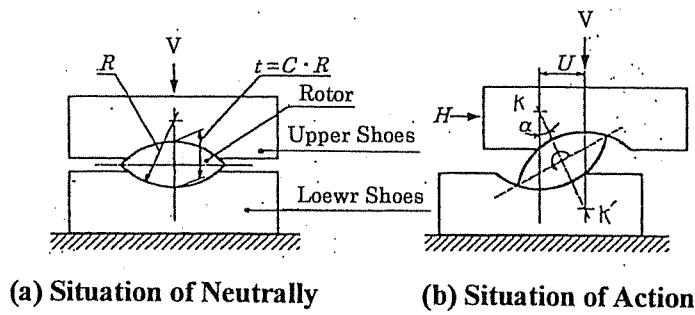


Figure-4

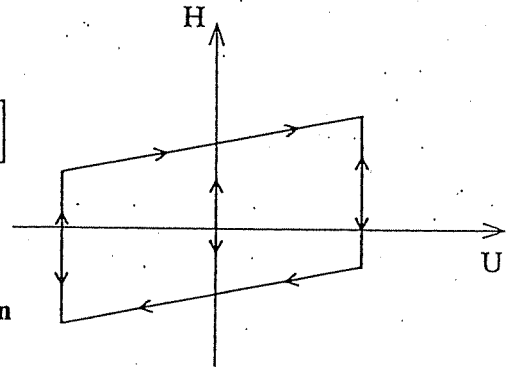


Figure-5

$$H = V \cdot \tan(\alpha + \rho) \quad \text{Eq (1)}$$

$$U = R \cdot (2 - C_B) \cdot \sin(\alpha) \quad \text{Eq (2)}$$

$$\alpha = \sin^{-1} \{u_B / R (2 - C_B)\} \quad \text{Eq (3)}$$

$$\sin \rho = 2 \cdot \mu / \{(2 - C_B) \cdot \sqrt{1 + \mu^2}\} \quad \text{Eq (4)}$$

$$C_B = t / R \quad \text{Eq (5)}$$

(H : Horizontal Load, V : Vertical Load, U : Horizontal Displacement, ρ : Coefficient by Eq (4), C_B : Coefficient by Eq (5), α : Turn Angle of Rotor, R : Radius of Rotor, t : Thickness of Rotor, u_B : Effective Displacement)

2.2 Verification of the device characteristics

To examine the hysteresis characteristics of the steel isolation bearing proposed in this paper, we made an experiment on vibrations by the sine wave, using a simple shaking table into which a seismic isolation device was incorporated. We verified Equations that assumes the hysteresis characteristics described in section "2.1". In addition, to further assess the characteristics of steel seismic isolation bearings, simulation by the finite element method (FEM) analysis was made.

Figure-6 compares the hysteresis curves obtained from the experiment with those of Equations and the results of the FEM analysis. The hysteresis curves of

Equations and the FEM results were computed using a friction coefficient of 0.25, because of the low pressure of the bearing surface. The hysteresis curves given by Equations agreed well with the experimental results, which proved the validity of the equations. At the same time, the FEM analysis showed a good reproduction of the experimental results.

2.3 Verification using a vibrating table

This experiment was made to cause a random sudden inertia force to act on a model structure on the shaking table. The model consisted of a mass corresponding to the superstructure and isolation bearings of steel. Actual seismic motions are so complicated and diverse

that fully simulating only using simple, continuing harmonic waveforms or waves of 1/2 cycle to one cycle with a great amplitude is impossible. Therefore, we found that understanding changes in input amplitude and cycle, and the aspects of transient vibrations that the structure responds to such changes, is necessary. The test was performed to reproduce the behavior of a model structure when receiving a sudden inertia force by using nonlinear dynamic analysis and the equivalent linear method and to obtain the constants used for theoretical equations.

1) Experimental method

Figure-7 shows a model structure and a shaking table. The table is placed on a linearway that is movable in a horizontal direction. An activator is provided by a lever to vibrate at a leverage of 1:3. Figure-8-21 show the results from the experiment and those of the simulation by the analysis, respectively.

By modeling from the theoretical equations and the dynamic analysis, the displacement behavior of the seismic isolation device was simulated almost accurately. From these results, the following were made clear.

- (a) The friction coefficient " μ " of polytetrafluoroethylene used for the theoretical equations of isolation bearings of steel was 0.1.
- (b) In the nonlinear dynamic analysis, a good approximation was attained by allowing for the viscosity coefficients " c " in the following two cases to reflect the velocity dependency of the friction coefficient:

- 1) where the sliding surface of pure polytetrafluoroethylene,

$$c = 35 \text{ kgf} \cdot \text{s/cm}$$

- 2) where the filler was included,

$$c = 5 \text{ kgf} \cdot \text{s/cm}$$

This agrees with the tendency in past reports¹¹⁾ that the latter case has a smaller velocity dependency than the former.

(c) The value of displacement response obtained by the equivalent linear method, which is commonly used as a design calculation method for seismic isolation bridges, is somewhat larger than the value obtained by the nonlinear dynamic analysis. Therefore this method gives a safer value than the actual value.

(d) The damping performance of the seismic isolation device, which has an almost rectangular hysteresis curve, such as a steel seismic isolation bearing, was found to be higher than that evaluated by the equivalent linear assumption.

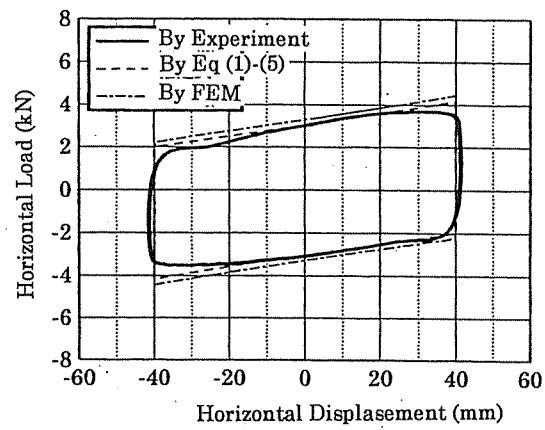


Figure-6 Hysteresis Curve

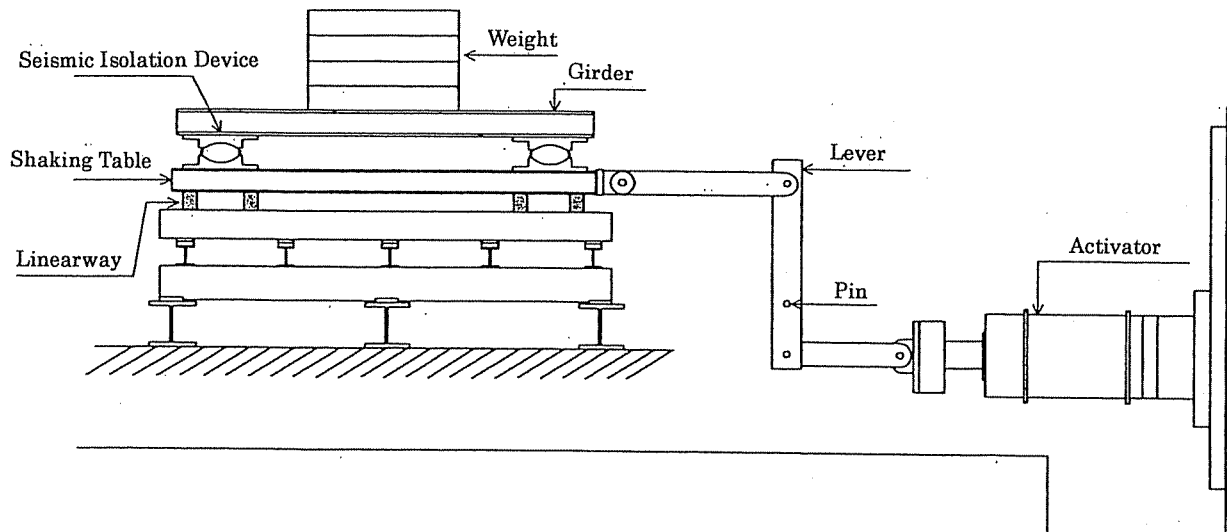


Figure-7 Model Structure and A Shaking Table

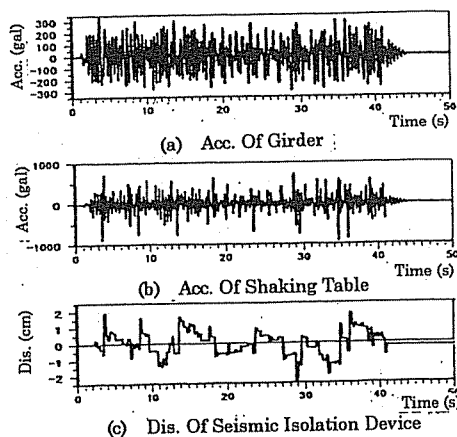


Figure-8 Experiment Value (Case A)
Input : Pink-Noise

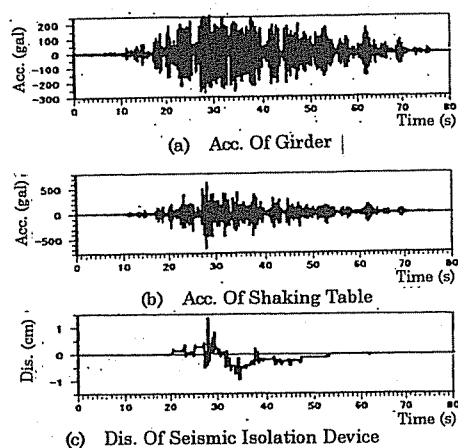


Figure-10 Experiment Value (Case A)
Input : Onnetou-Oohashi

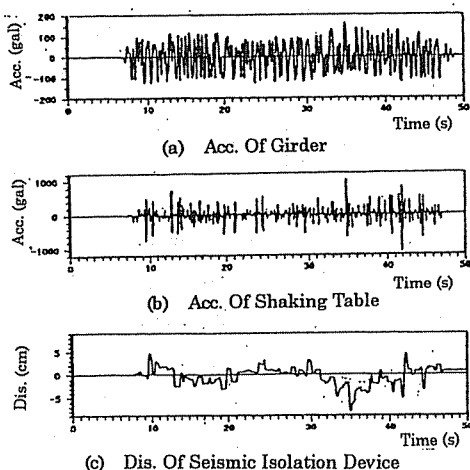


Figure-12 Experiment Value (Case B)
Input : Pink-Noise

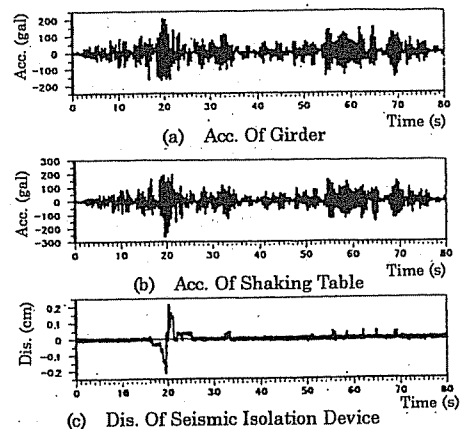


Figure-9 Experiment Value (Case A)
Input : Simulated Earthquake

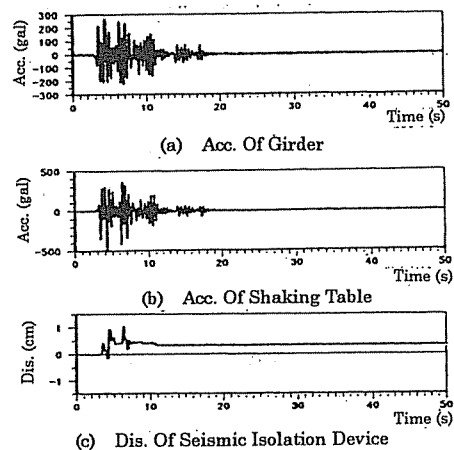


Figure-11 Experiment Value (Case A)
Input : Kobe Marine Observatory

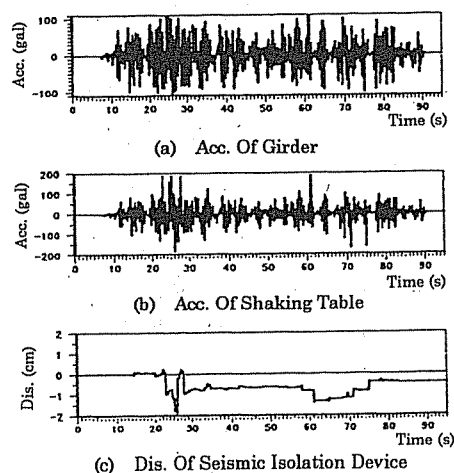


Figure-13 Experiment Value (Case B)
Input : Simulated Earthquake

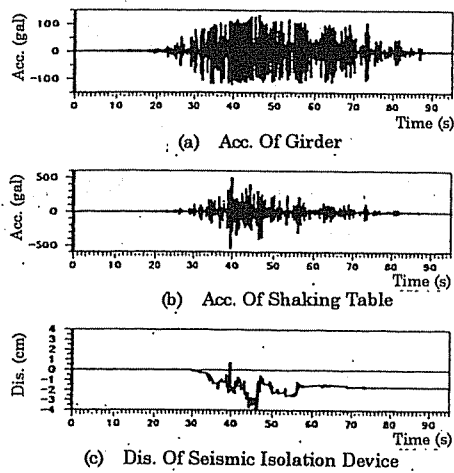


Figure-14 Experiment Value (Case B)
Input : Onnetou-Oohashi

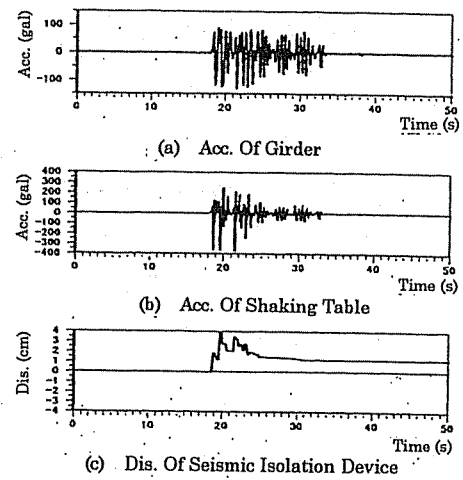


Figure-15 Experiment Value (Case B)
Input : Kobe Marine Observatory

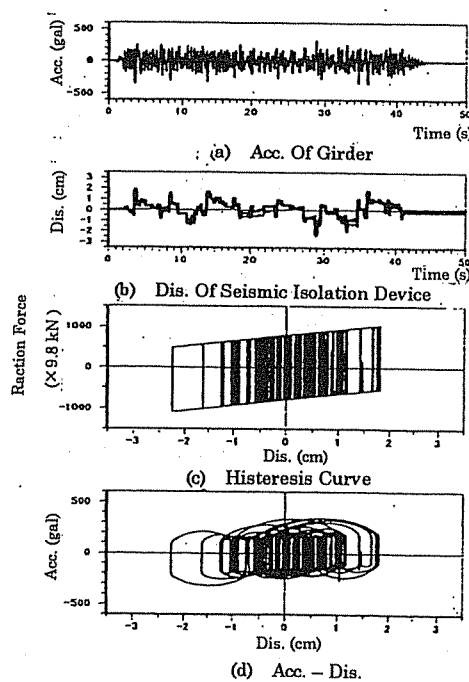


Figure-16 Nonlinear Dynamic Analysis
(Case A)

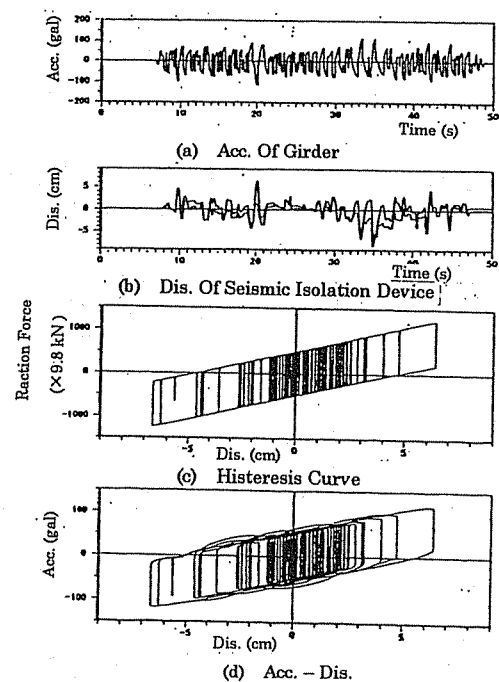
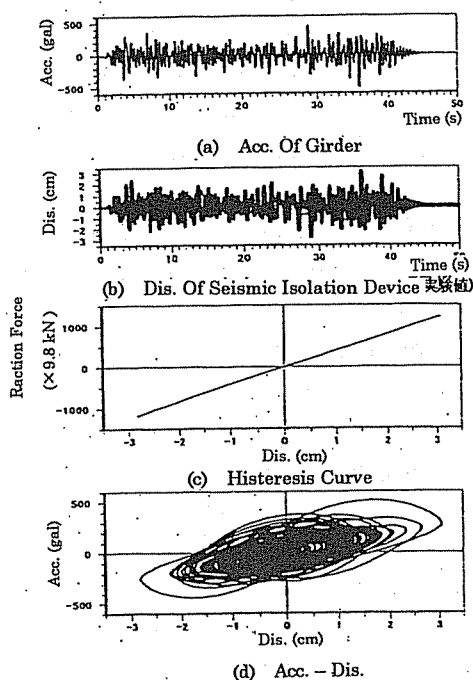
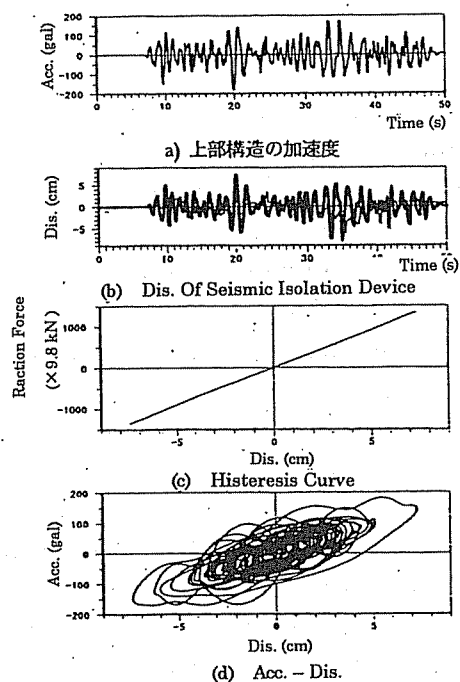


Figure-17 Nonlinear Dynamic Analysis
(Case B)



**Figure-18 Equivalent Liner Method
(Case A)**



**Figure-19 Equivalent Liner Method
(Case B)**

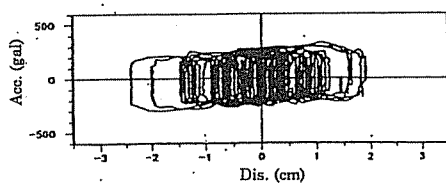


**Figure-20 Hysteresis Curve By Experiment
(Case A)**

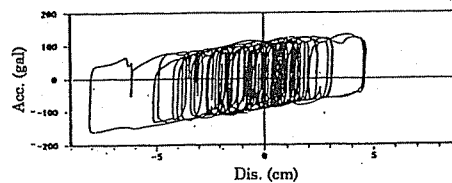


**Figure-21 Hysteresis Curve By Experiment
(Case B)**

3. EXPERIMENT USING AN ALMOST FULL-SCALE MODEL BRIDGE

3.1 An experiment using steel bridge piers for substructure

To confirm the performance level of seismic isolation bearings of steel required for a real bridge we made a dynamic loading test using a full-scale two-span continuous girder and steel piers. Seismic isolation bearings and pin bearings were used to investigate and compare their response behavior.

3.1.1 Experimental method

The configuration of the experimental equipment was a superstructure, two abutments, two bearings, two pier models, a substructure (pallet), an air bearing, an abutment test wall and foundation (Figure-22). The movable part of the equipment of total weight 3340 kN was made collide against the abutment test wall. The Superstructure was a two-span continuous girder bridge (span: 15.0m \times 2, interval of main girder: 1.8m, H-steel 2 main girders). The ends of the main girders of the superstructure were supported on the abutments by two rollers that moved the girders. The two steel piers supported the superstructure by a bearing in the middle. Because the weight of the superstructure was 1025 kN, and because the effective span was uniform, the dead load on a middle supports was 5/8 of the total, or 640 kN.

The steel pier with a circular cross section (Figure-23) was used for the substructure. To save on costs, ready-made steel pipes (STK 400) were used for

the columns of pier, while SM 400 were provided for all steel plate members other than the columns because of their weldability. The yield strength of the steel pipes used was 259 MPa. The sectional size of pier was determined so that the pier base could yield at a response acceleration of about 1 G.

We experimented with the following two bearings: 1) steel seismic isolation bearings, and 2) pin bearings. The steel seismic isolation bearing had a curvature radius of the rotating plate (R) = 30 cm and a thickness (t) = 18 cm (Figure-24). PTFE having a diameter of 3 cm were concealed as contact members in the upper and lower shoes of the seismic isolation bearing (30 each). The friction coefficient between the PTFE and the rotating plate was about 0.11, and the hysteresis characteristics of a seismic isolation bearing are given by Equations (1) - (5) and are represented by the curve in Figure-25.

In the experiment, the substructure to which the pier was fixed was caused to run by dropping a 98-kN weight and to collide against the abutment test wall. At this time, input acceleration provided for the substructure was adjusted by changing the distance traveled by the substructure and the thickness of shock absorbing material (expanded polystyrene form).

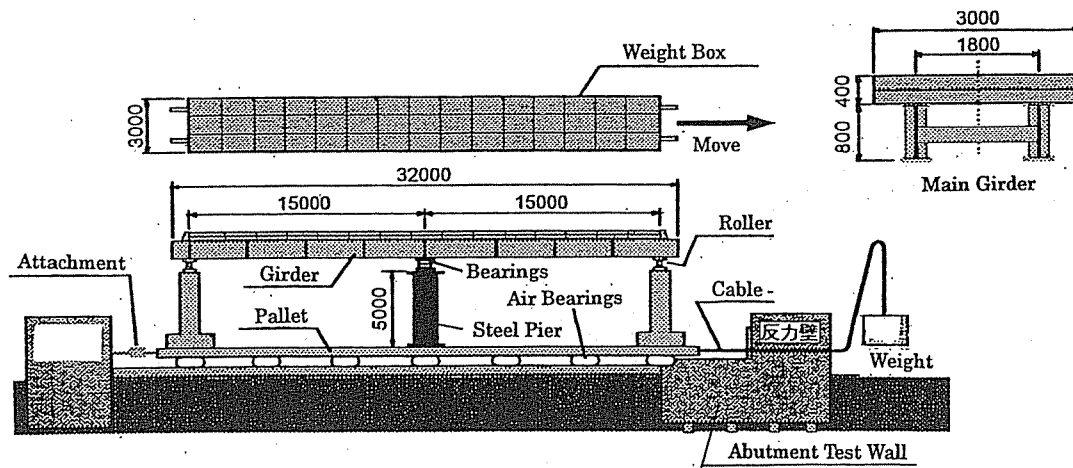


Figure-22 Experiment Equipment

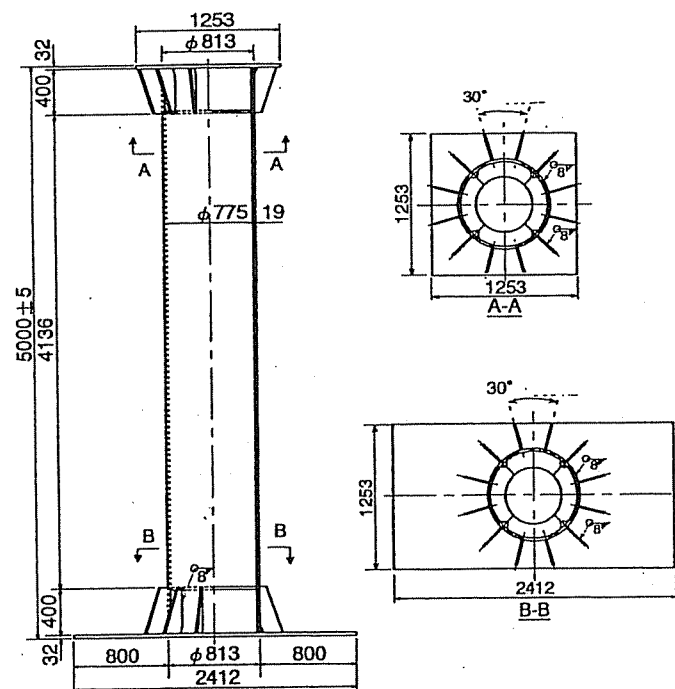


Figure-23 The Steel Pier

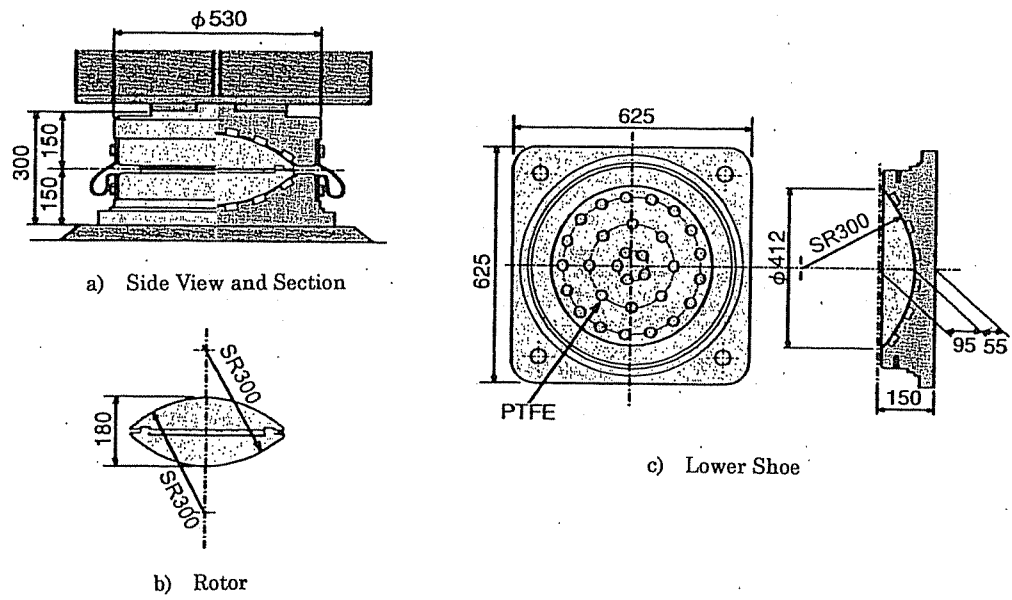


Figure-24 Seismic Isolation Bearings of Steel

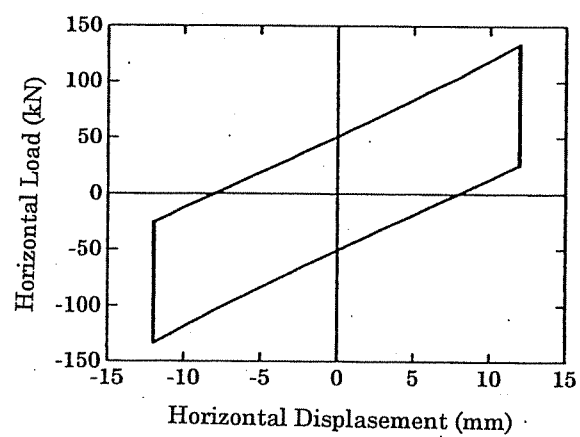


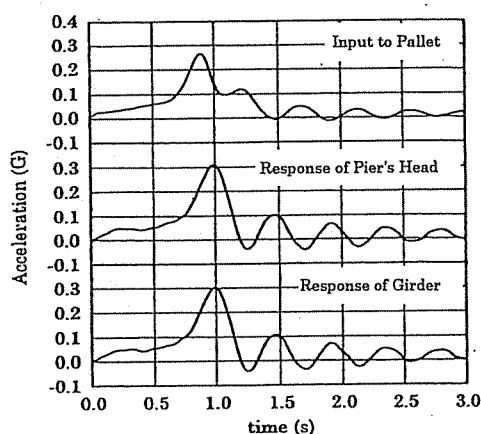
Figure-25 Histeresis Curve

3.1.2 Experimental results

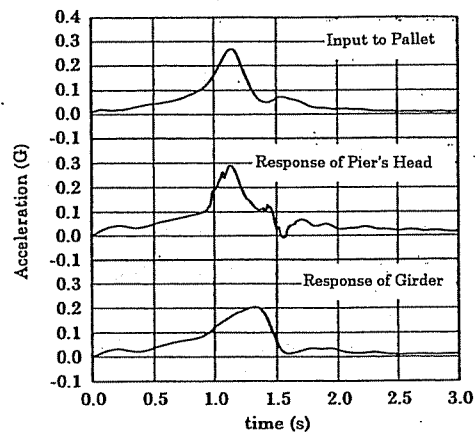
Figure-26 shows an example of the input and the response acceleration wave forms that compares the steel seismic isolation bearings and pin bearings. When pin bearings were used, the wave forms of the response accelerations of the upper ends of the pier and the superstructure were almost the same, and the maximum value increased by about 10%, compared with that of the input acceleration. In addition, free vibration with the natural frequency of the system occurred after the collision. However, when the steel seismic isolation bearing was used, the response acceleration of the superstructure

greatly decreased compared with that of input acceleration. Moreover, the vibration after the collision was reduced.

Figure-27 shows the relationship between the maximum input acceleration and the amplification factor under all conditions in the experiment. Here, the amplification factor was defined as the ratio of the maximum response acceleration of the superstructure to the maximum input acceleration. With the steel seismic isolation bearings, the response amplification was always a value of less than 1.0, a decrease of about 30 %, compared with the pin bearings.



(a) Pin Bearing



(b) Steel Seismic Isolate Bearing

Figure-26 Acceleration Wave Forms

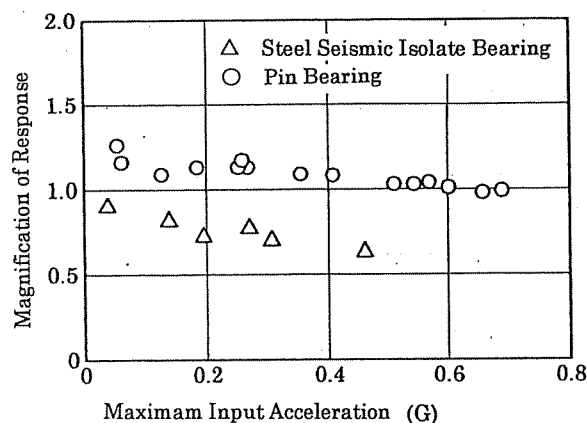


Figure-27 Input Acceleration And Magnification of Response

3.2 Experiment using substructure of reinforced concrete.

3.2.1 Model structure and measurements

The model structure was the wall type pier model (Figure-28) designed from earthquake-resistant design criteria. The wall had a thickness of 80 cm, a width of 250 cm and a height of 400 cm. The *dan-otoshi* was, or the reinforcement ratio of the pier changed, at a height of 150cm from the wall base.

The accelerations and strain of reinforcing bars were measured: accelerometers measuring the horizontal direction were installed on the side of the wall at every 50cm from the base, while those measuring the vertical and horizontal directions were attached to the center of the girders. Strain gauges to measure the main reinforcement were also attached on tension side and compression side of two reinforcing bars, respectively, at every 50cm from the base. The strain frequency of the measurements in the sampling was 1 kHz.

3.2.2 Experimental results

In this experiment, the model structure showed elastic behavior because a loading test up to the ultimate state was unable to be performed, because of experimental circumstances. Figure-29 shows the input acceleration, the response acceleration of the pier crown, and the response acceleration of the superstructure under this experimental condition.

The response acceleration of the pier

crown reached the maximum acceleration having a response value of about 2G almost at the same time as the maximum input acceleration, while the superstructure reached the maximum response 0.3 sec. later than the peak input acceleration. This maximum response showed a small value of 0.4G. In an experiment using pin bearings with the model structure of the same design, when the response accelerations of the pier crown and the superstructure were about 1.3G, flexural and shear failure were observed at the *dan-otoshi* where the reinforcement ratio of the pier changed. However, in our experiment, no damage was found in the model structure using the seismic isolation bearing. From these facts, we found that the seismic isolation bearing functions even when a sudden inertia force acts on the model structure. The inertia force that acts on the superstructure can be reduced by using the steel seismic isolation bearings, and thus damage to piers can be appreciably mitigated by changing the bearings of existing bridges to the steel seismic isolation bearings.

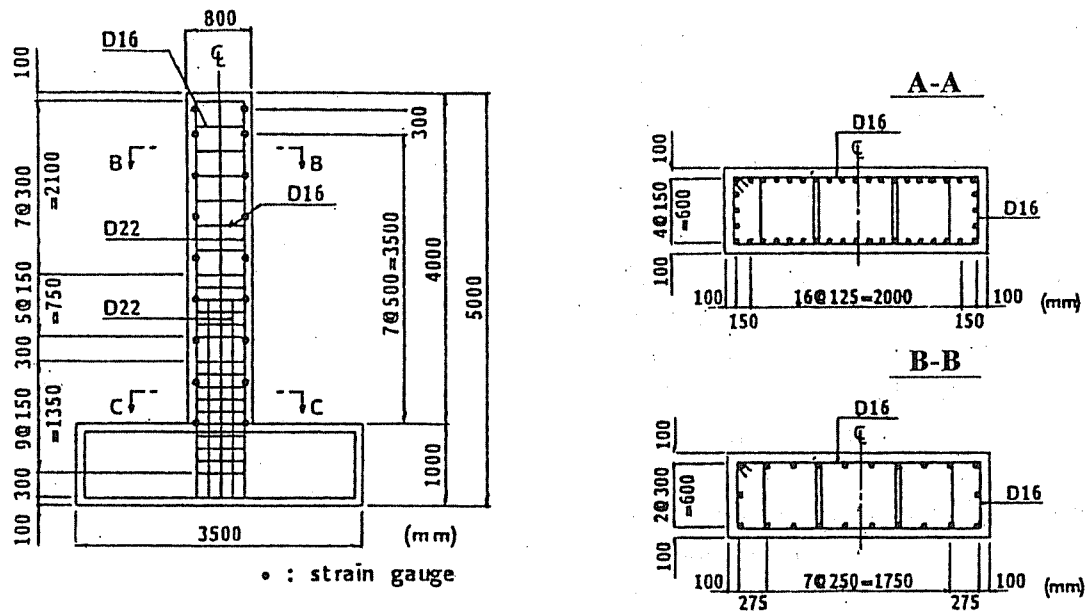


Figure-28 Model Structure

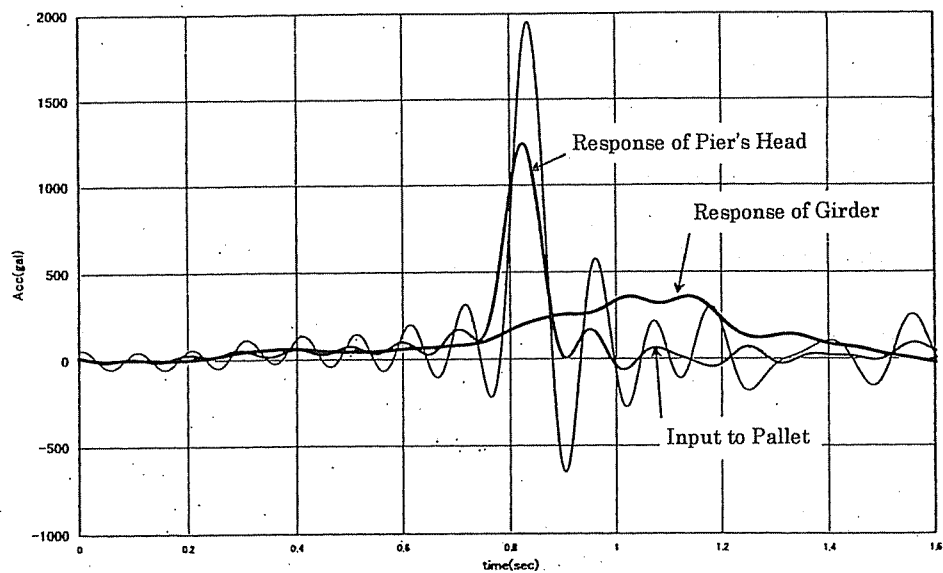


Figure-29 Acceleration Wave Forms

4. CONCLUSIONS

The experimental equipment of the air cushion made it possible to produce an acceleration of approximately 1.0G with almost full-scale model structures. Success in generating such a strong inertia force by a relatively low-cost equipment has provided the designers with opportunities to verify their design.

From the hysteresis curves, seismic isolation equipment that uses very large values of friction yield hysteresis reduction, and to reduce natural free vibrations of a structure. It also has an effect of reducing such an impact inertia force that was generated by the equipment used in our experiment. Thus it greatly contributes to not only the efforts to improve the effect of seismic isolation design, but also to its use in cold regions.

In the experiment using the steel pier columns, the responses of pin bearings and steel seismic isolate bearings were compared using the pin bearings and steel seismic isolate bearings. The result was that the response decreased by about 30 % when the steel seismic isolate bearings were used, which proved the effectiveness of steel seismic isolate bearings against the seismic impact.